Reversible alternation between bipolar and unipolar resistive switching in La-$SrTiO_3$ thin films*

Xu Ding-Lin(许定林)[a], Xiong Ying(熊 颖)[b], Tang Ming-Hua(唐明华)[a]†, Zeng Bai-Wen(曾柏文)[a], Xiao Yong-Guang(肖永光)[a], and Wang Zi-Ping(王子平)[a]

[a] *Key Laboratory for Low Dimensional Materials and Application Technology of Ministry of Education, Xiangtan University, Xiangtan* 411105, *China*
[b] *School of Mathematics and Computational Science, Xiangtan University, Xiangtan* 411105, *China*

(Received 4 March 2013; revised manuscript received 9 April 2013)

The alternation from bipolar to unipolar resistive switching is observed in perovskite $La_{0.01}Sr_{0.99}TiO_3$ thin films. These two switching modes can be activated separately depending on the compliance current (I_{comp}) during the electro-forming process: with a higher I_{comp} (5 mA) the unipolar resistance switching behavior is measured, while the bipolar resistance switching behavior is observed with a lower I_{comp} (1 mA). On the basis of *I–V* characteristics, the switching mechanisms for the URS and BRS modes are considered as being a change in the Schottky-like barrier height and/or width at the Pt/La-$SrTiO_3$ interface and the formation and disruption of conduction filaments, respectively.

Keywords: unipolar and bipolar resistive switching, La-doped $SrTiO_3$ thin film

PACS: 73.61.Ng, 72.80.Ga **DOI:** 10.1088/1674-1056/22/11/117314

1. Introduction

Resistance random access memory (RRAM) has attracted a great deal of attention in recent years due to its low power consumption, long retention time, small cell size, fast operation, low cost, high endurance, non-destructive readout, and simple device structure. Two schemes have been defined related to the electrical polarity required for resistive switching. When the resistance change does not depend on the polarity of the voltage or current and the device can be switched between high resistance state (HRS) and low resistance state (LRS) with the same polarity, this polarity-independent switching behavior is called unipolar resistance switching (URS). The second scheme is called bipolar resistance switching (BRS) because polarity opposite to that of the applied voltage is needed to switch between HRS and LRS.[1–4] These resistive switching phenomena have been observed in a wide variety of binary transition metal oxides such as Cu_xO, ZnO, TiO_2, ZrO_2,[5–9] perovskite oxides such as $SrZrO_3$, $BiFeO_3$, $SrTiO_3$,[10–12] as well as silicon oxides,[13] etc.

It would be advantageous to have both BRS and URS schemes in the same material. For ZnO[6] and TiO_2[8] thin films, a permanent transition from BRS to URS has been observed. Shen *et al.* reported that reversible switching between the two switching schemes occurs in Mn doped $BaSrTiO_3$ thin films when the switching voltage is varied across a threshold voltage.[14] However, a report of controlling the reversible switching between the two switching schemes by means of the compliance current and switching voltage is still lacking in the literature. In this article, we report the reproducible transformation between bipolar and unipolar resistive switching obtained with different compliance currents in 1% La doped $Sr_{0.99}TiO_3$ (La-STO) perovskite thin films deposited between Pt electrodes with the sol–gel method.[15]

2. Experimental details

Strontium acetate ($SrC_4H_6O_4{\cdot}1/2H_2O$, AR, 99.9%) and lanthanum acetate hydrate ($C_6H_9O_6La{\cdot}1/2H_2O$, AR, 99.99%) were added into the acetic acid (AR, 99.5%) in the right amounts. The mixture was stirred at 60 °C for 30 min to dissolve the solute into the solvent, forming clear solution A. Then, the acetylacetone (AR, 99.5%) and the titanium butoxide ($Ti(OC_4H_9)_4$, AR, 99%) were added into methoxyethanol (AR, 99.5%), forming solution B. Subsequently, solutions A and B were mixed. Some amounts of ethylene glycol (AR, 99.5%) and glycerol (AR, 99.5%) were successively added to the mixed solution. The mixture was stirred at 60 °C for 60 min for reacting completely to form the final solution. The prepared 0.2 M precursor solution was spin-coated on the Pt/Ti/SiO_2/Si substrates with the stock solution at 500 rpm/4000 rpm for 10 s/30 s to form a sol–gel film. After baking at 180 °C for 5 min, the as-deposited layer was heat-treated

*Project supported by the Key Projects of the National Natural Science Foundation of China (Grant No. 11032010), the National Natural Science Foundation of China (Grant Nos. 51072171, 61274107, 61176093, and 11275163), the Program for Changjiang Scholars and Innovative Research Team in University, China (Grant No. IRT1080), the National Basic Rearch Program of China (Grant No. 2012CB326404), the Key Projects of Scientific Research Fund of Hunan Provincial Education Department, China (Grant No. 12A129), the Doctoral Program of Higher Education of China (Grant No. 20104301110001), and the Aid Program for Science and Technology Innovative Research Team in Higher Educational Institutions of Hunan Province, China.

†Corresponding author. E-mail: mhtang@xtu.edu.cn

© 2013 Chinese Physical Society and IOP Publishing Ltd

at 380 °C for 10 min. The coating and heating steps were repeated 4 times, and then the samples were annealed at 700 °C for 10 min in air. The measured thicknesses of La-$SrTiO_3$ thin films were approximately 200 nm. Finally, the top electrodes of Pt were sputtered onto the deposited thin films by ion sputtering through a shadow mask to define circle-shaped electrodes with a thickness of 300 nm and a diameter of 200 μm.

The electrical measurement was performed with a Keithley 4200-SCS semiconductor parameter analyzer (USA). A schematic drawing of the measurement configuration is shown in the inset of Fig. 1. In the *I*–*V* measurements, the voltage bias that drives current flowing from the top Pt electrode to the La-STO is defined as positive.

3. Results and discussion

Figure 1 shows the X-ray diffraction (XRD) pattern of the La-STO thin films annealed at 700 °C. The three diffraction peaks can be indexed to (110), (211), and (200) of La-STO, indicating that the thin films are polycrystalline. The (110) XRD peak is clearly observed.

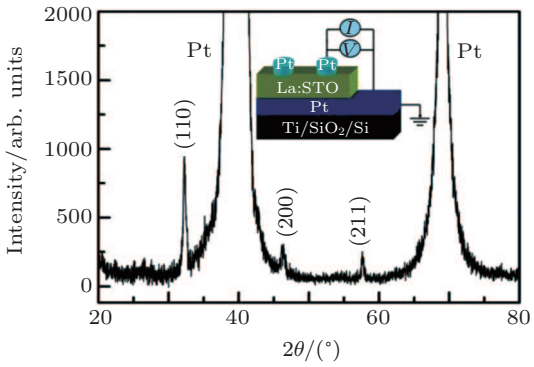


Fig. 1. (color online) XRD θ–2θ scan results of La-STO films grown on Pt(120 nm)/Ti/SiO_2/Si substrates.

The URS behavior has been measured in the sandwich (MIM) structure of Fig. 1. The compliance current I_{comp} increases to 5 mA, electroforming occurs at +5.5 V of the positive branch and the device is transformed to have a better conducting and linear behavior, as can be seen in Fig. 2. The first resistance switching from the initial state to LRS is called the electroforming process, which is a necessary initial process for unipolar resistive switching. When the voltage is swept to +0.8 V with $I_{comp} = 10$ mA, the current drops abruptly, which means that the device is switched from the unipolar LRS to the unipolar HRS (reset process). After setting $I_{comp} = 5$ mA and the sweep voltage to 3.5 V (smaller than the electroforming voltage), the current jumps and the device is switched back to LRS again (set process). The ratio of HRS to LRS is more than 10^3. By setting $I_{comp} = 1$ mA and increasing the sweep voltage to +3.2 V, the HRS switches to LRS again and the reset voltage is +1.1 V. The set and reset currents change little with different compliance currents and are different from the previous reports.[16,17]

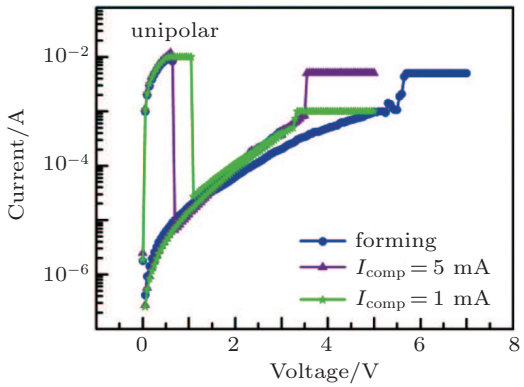


Fig. 2. (color online) The URS behaviors with $I_{comp} = 5$ mA, 1 mA in the Pt/La-STO/Pt device.

The I_{comp} is an important parameter for the electroforming process.[18] Different I_{comp} is critical for the formation of different switching modes. The electroforming into the URS or BRS mode is completed with 5 mA or 1 mA, respectively. Figure 3 shows the electroforming processes with $I_{comp} = 5$ mA (green line) and $I_{comp} = 1$ mA (blue line). Set $I_{comp} = 1$ mA, the current direction from the top electrode is defined as positive and the opposite one is defined as negative. The *I*–*V* hysteresis loop is measured with the order of -3 V$\rightarrow$ 0 V$\rightarrow$ +3 V$\rightarrow$ -3 V. In Fig. 3, the blue line shows the electroforming process in BRS. Set $I_{comp} = 0.5$ mA, the voltage is swept in a sequence of -5 V$\rightarrow$ 0 V$\rightarrow$ +5 V$\rightarrow$ -5 V again in Fig. 4(a). When the positive bias voltage is +1.2 V, the leakage current density increases from HRS to LRS. When the negative bias voltage is -1 V again, the leakage current density abruptly drops and the switching mode changes from LRS to HRS. But when the sweep voltage is swept to -3.5 V, the leakage current density increases again, just like the set process (arrows 7 and 8) in unipolar. The set voltage in bipolar is smaller than that in unipolar behavior. Upon setting $I_{comp} = 0.1$ mA, the *I*–*V* hysteresis loop is measured with the order of -1.5 V$\rightarrow$ 0 V$\rightarrow$ +1.5 V$\rightarrow$ -1.5 V. In Fig. 4(b), when the bias voltage is +1.2 V, the leakage current density increases from HRS to LRS. When the negative bias voltage is -0.9 V again, the leakage current density abruptly drops and the mode changes from LRS to HRS. Consequently, we can obtain either BRS or URS by controlling the switching voltage and compliance current. This bipolar to unipolar transition is dynamically repeatable. Moreover, when the sweeping voltage and I_{comp} are decreased, the unipolar switching can be converted to the bipolar switching again as illustrated in Fig. 4(a).

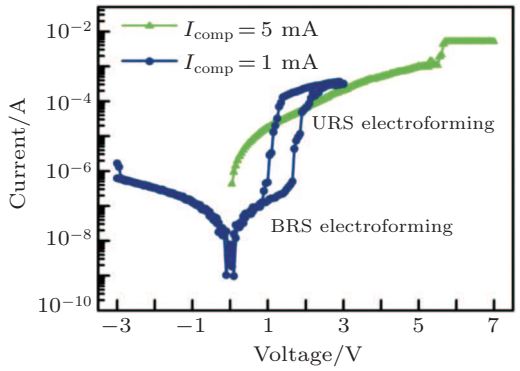


Fig. 3. (color online) Electroforming process with $I_{comp} = 1$ mA, which results in the BRS mode, and that with $I_{comp} = 5$ mA, which results in the URS mode.

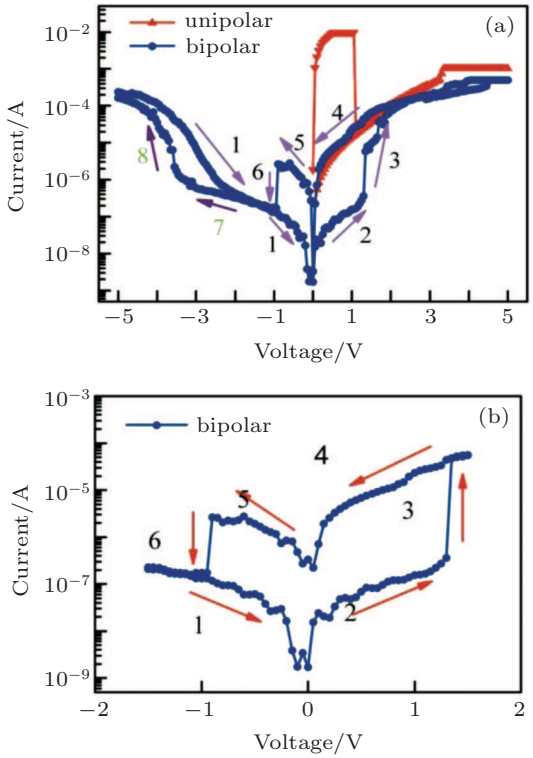


Fig. 4. (color online) (a) BRS behaviors with high voltage (5 V), the LRS in bipolar switching works as the HRS in the unipolar switching mode. (b) BRS behaviors with low voltage (1.5 V).

Figures 5(a) and 5(b) show the resistance evolution of the HRS and LRS within 50 switching cycles. The resistance values of the two states are read out at 0.4 V in each switching cycle. The resistance ratio of HRS to LRS is as high as 10^3 for the URS mode, and the resistance ratio of HRS to LRS is approximately 10^2 for the BRS mode. As can be seen from Fig. 5, the HRS of the URS mode is approximately the LRS of the BRS mode, therefore a multilevel capability could be achieved in this device.[9] And both modes show little degradation during the 50 repeated sweep cycles. The insets in Figs. 5(a) and 5(b) show the switching voltage distributions of 50 cycles for URS and BRS modes, respectively. The threshold voltages in the two modes are relatively small, especially for BRS, which is beneficial to low voltage applications. From these measurement results, we conclude that the La-STO device is highly controllable, reversible, and reproducible for nonvolatile memory applications.

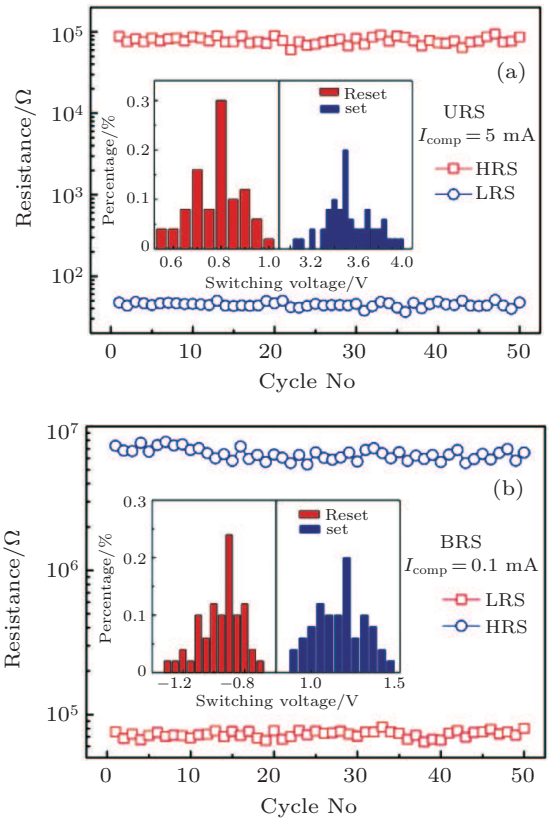


Fig. 5. (color online) Resistance evolution of the HRS and LRS of the (a) URS and (b) BRS in 50 cycles. The insets show the distributions of set and reset voltages of the (a) URS and (b) BRS.

It should be noted that, as described Ref. [14], if the current compliance used in the first forming is sufficient to completely reach the metallic LRS shown in Fig. 6(a), the device will directly show unipolar switching. Accordingly, the first forming current is of great importance and the metallic LRS is the prerequisite for the observation of unipolar switching in polycrystalline La-STO thin films. However, if the first forming current does not reach the metallic LRS of the unipolar switching mode, bipolar switching can be carried out by sweeping negative and positive voltages. Thus, different I_{comp} is critical for the formation of different switching modes.

The alternation between BRS and URS has been observed in perovskite La-STO thin films. When the sweeping voltage and I_{comp} are decreased, the URS mode can be converted to the BRS mode, while the sweeping voltage and I_{comp} are increased, the BRS mode switches to the URS mode. A reasonable mechanism for this alternation can be described as follows. After the unipolar set process, there will be a conductive filament consisting of oxygen vacancies formed in between the top and the bottom electrodes, and in the reset process, the filament will not be complete but will be locally ruptured.[14]

Thus, when the sweeping voltage is swept to negative, the oxygen vacancies are reduced by oxygen ions from the Pt and bulk interface. The conductive filament consisting of oxygen vacancies is ruptured, the HRS in the unipolar switching mode is converted to the HRS in the bipolar switching mode. Therefore, in the following I–V sweep, the bipolar switching mode can be realized by controlling the low sweep voltage and a lower $I_{\rm comp}$, which is different from the previous reports.[14] For the transition from the bipolar switching mode to the unipolar switching mode, when the sweeping voltage is close to 1.5 V, the oxygen ions migrate to the top electrode, leaving the oxygen vacancies to form tiny filaments, lowering the Schottky barrier, and the device is switched into the LRS of the bipolar switching mode (HRS of unipolar switching mode). Subsequently, if we increase the $I_{\rm comp}$, these tiny conducting filaments will gather together to form stronger and more conductive filaments, leading to the transition to the LRS under the larger positive sweeping voltage. The unipolar switching mode is thus obtained.

To further understand the conduction and switching mechanisms of the RRAM device, the I–V characteristics are replotted as ln$I$–ln$V$ and ln$I$–$V^{1/2}$. Figure 6(a) shows the logarithmic plot and linear fitting of the previous I–V curve in unipolar for the positive voltage sweep region; it is similar for the negative branch. As shown in Fig. 6(a), the I–V relationship in LRS clearly exhibits an Ohmic conduction behavior with a slope of 0.94, which is regarded as the formation of conductive filaments in the device during the set process. However, the conduction mechanism in the HRS is much more complicated. The fitting results for the HRS show that the charge transport behavior is in good agreement with the classical trap-controlled space charge limited conduction (SCLC),[19] which consists of three portions: the Ohmic region (slope = 1.16), the Child's law region (slope = 2.18), and the steep current increase region. The totally different conduction behaviors in LRS and HRS also suggest the formation of strong filaments that switch the film to the LRS mode. By setting a higher $I_{\rm comp}$, the film switches back to the HRS, also indicating that this is due to the rupture of the filaments caused by the heat generated by the large current flow. So the filamentary model can be used to explain the URS phenomenon of the thin film.

As shown in Fig. 6(b), the HRS in bipolar switching has a linear fitting only at the ln$I$ versus square root voltage plot with a slope of 3.63, fitting with the Schottky mechanism. On the other hand, the LRS in bipolar switching also is in good agreement with the classical trap-controlled space charge limited conduction. As a result, the LRS in bipolar switching works as the HRS in the unipolar switching mode in the same voltage sweep region (0 V$\rightarrow$ +1.5 V). A possible origin for the resistance switching is the change of the Schottky barrier height (or width) at the interface.[20,21] Defects such as oxygen vacancies and interstitial atoms inevitably exist in polycrystalline thin films. The oxygen ions are concentrated at the top interface after the electroforming with $I_{\rm comp} = 0.1$ mA. The oxygen ions are accumulated (extracted) into (from) the interface region upon a positive (negative) bias, which leads to a change in the Schottky-like barrier width and/or height during voltage sweeping.

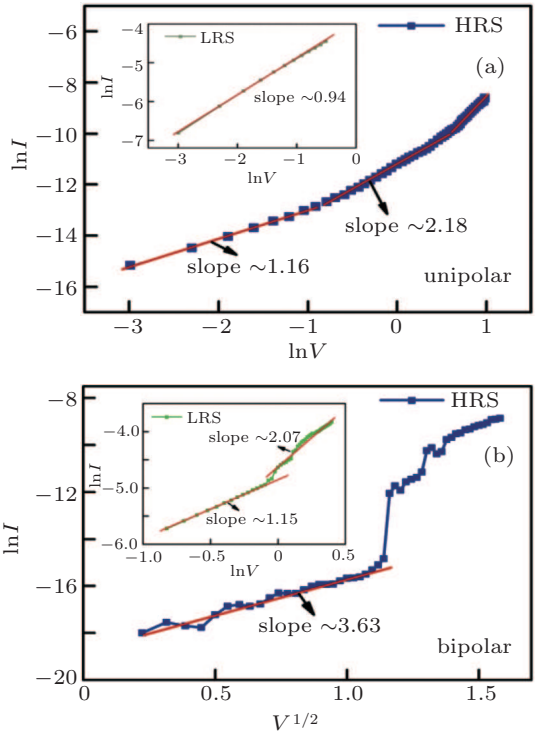


Fig. 6. (color online) (a) The ln$I$–ln$V$ curves of a URS memory. (b) The ln$I$–$V^{1/2}$ curves of a BRS memory. The insets show the I–V curves of LRS.

The SCLC conduction mechanism is the bulk effect, while the Schottky mechanism is the metal/insulator interfacial effect. From these results, we explain the mechanisms of BRS and URS of the polycrystalline La-STO thin film using the metal/insulator interfacial effect and the bulk effect, respectively.

4. Conclusion

In summary, we have observed a reversible alternation of bipolar and unipolar resistive switching in a Pt/La-STO/Pt cell. More specifically, setting a high compliance current leads to unipolar resistive switching, and setting a low compliance current leads to bipolar resistive switching. According to the electrical results, a modification of the Schottky emission in the interface is considered to be the mechanism for the BRS, while the filaments' conduction is evident for the URS. The conversion between BRS and URS is reversible by controlling different $I_{\rm comp}$ levels and voltage ranges, respectively. The LRS of the bipolar switching state is identical with the HRS of

the unipolar switching state. This study also introduces the importance of the compliance current in resistance switching phenomena.

References

[1] Meijer G I 2008 *Science* **319** 1625
[2] Waser R and Aono M 2007 *Nature Mater.* **6** 833
[3] Yang Y C, Pan F, Liu Q, Liu M and Zeng F 2009 *Nano Lett.* **9** 1636
[4] Liu Q, Long S B, Wang W, Zuo Q Y, Zhang S, Chen J N and Liu M 2009 *IEEE Electron Device Lett.* **30** 1335
[5] Lv H B, Zhou P, Fu X F, Yin M, Song Y L, Tang L, Tang T A and Lin Y Y 2008 *Chin. Phys. Lett.* **25** 1087
[6] Lee S, Kim H, Park J and Yong K 2010 *J. Appl. Phys.* **108** 076101
[7] Zhao J W, Liu F J, Huang H Q, Hu Z F and Zhang X Q 2012 *Chin. Phys. B* **21** 065201
[8] Jeong D S, Schroeder H and Waser R 2007 *Electrochem. Solid-State Lett.* **10** G51
[9] Liu M, Abid Z, Wang W, He X L, Liu Q and Guan W H 2009 *Appl. Phys. Lett.* **94** 233106
[10] Liu Y C, Chuang C C, Chen J S, Wang A, Jang W Y, Young J C, Chiu K Y and Tseng T Y 2006 *Thin Solid Films* **494** 287
[11] Li M, Zhuge F, Zhu X J, Yin K B, Wang J Z, Liu Y W, He C L, Chen B and Li R W 2010 *Nanotechnology* **21** 425202
[12] Szot K, Speier W G, Bihlmayer G and Waser R 2006 *Nature Mater.* **5** 312
[13] Wang Y, Liu Q, Lv H B, Long S B, Zhang S, Li Y T, Lian W T, Ynag J H and Liu M 2011 *Chin. Phys. Lett.* **28** 077201
[14] Shen W, Dittmann R and Waser R 2010 *J. Appl. Phys.* **107** 094506
[15] Lee C, Kim I, Shin H, Kim S and Cho J 2009 *Langmuir.* **25** 11276
[16] Rohde C, Choi B J, Jeong D S, Choi S, Zhao J S and Hwang C S 2005 *Appl. Phys. Lett.* **86** 262907
[17] Lee S B, Kim A, Lee J S, Chang S H, Yoo H K, Noh T W, Kahng B, Lee M J, Kim C J and Kang B S 2010 *Appl. Phys. Lett.* **97** 093505
[18] Sun X W, Li J Q, Zhang X A, Ding L H and Zhang W F 2011 *J. Phys. D: Appl. Phys.* **44** 125404
[19] Lampert M A 1956 *Phys. Rev.* **103** 1648
[20] Kim H, Park C, Lee S and Kim D W 2009 *J. Phys. D: Appl. Phys.* **42** 055306
[21] Fujii T, Kawasaki M, Sawa A, Akoh H, Kawazoe Y and Tokura Y 2007 *Phys. Rev. B* **75** 165101